o = arbitrary position at base of far field region, membrane surface
r = radial
w = surface of disk; wall
z = axial
ϕ = circumferential
∞ = position of far-radial or far-axial boundary condition

LITERATURE CITED

Bödewadt, V. T., "Die Drehströmung über festem Grunde," Z. *Angew. Math. Mech.*, **20**, 241 (1940).

Carslaw, H. S., and J. C. Jaeger, Conduction of Heat in Solids, 2nd Edit., Oxford University Press, Oxford (1959).

Chan, W. C., and L. E. Scriven, "Absorption into Irrotational Stagnation Flow. A Case Study in Convective Diffusion Theory," *Ind. Eng. Chem. Fundamentals*, **9**, 114 (1970).

Cochran, W. G., "The Flow Due to a Rotating Disk," *Proc. Camb. Phil. Soc.*, **30**, 365 (1934).

Colton, C. K., "Permeability and Transport Studies in Batch and Flow Dialyzers with Applications to Hemodialysis," Ph.D. thesis, Mass. Inst. Technol., Cambridge (1969).

———, K. A. Smith, P. Stroeve, and E. W. Merrill, "Laminar Flow Mass Transfer in a Flat Duct with Permeable Walls," *AIChE J.*, **17**, 773 (1971).

Colton, C. K., and K. A. Smith, "Mass Transfer to a Rotating Fluid. Part II. Transport from the Base of an Agitated Cylindrical Tank," *ibid.*, **18**, 958 (1972).

Dorfman, L. A., 'Hydrodynamic Resistance and the Heat Loss of Rotating Solids, Oliver and Boyd, London (1963).

Greenspan, H. P., The Theory of Rotating Fluids, Cambridge Univ. Press, Cambridge (1968).

von Karman, T., "Laminaire und turbulente Reibung," Z. *Angew. Math. Mech.*, **1**, 233 (1921).

Levich, V. G., Physicochemical Hydrodynamics, Prentice-Hall, Englewood Cliffs, N. J. (1962).

Lugt, H. J., and E. W. Schwiderski, "Temperature Distributions in Rotating Flows Normal to a Flat Surface," *Quart. J. Mech. Appl. Math.*, **23**, 133 (1965).

Mack, L. M., "The Laminar Boundary Layer on a Disk of Finite Radius in a Rotating Flow. Part I: Numerical Integration of the Momentum-Integral Equations and Application of the Results to the Flow in a Vortex Chamber," Jet Propulsion Lab. Techn. Rept. No. 32-224 (May, 1962).

———, "The Laminar Boundary Layer on a Disk of Finite Radius in a Rotating Flow. Part II: A Simplified Momentum-Integral Method," No. 32-366 (Jan. 1963).

Millsaps, K., and K. Pohlhausen, "Heat Transfer by Laminar Flow from a Rotating Plate," *J. Aeronaut. Sci.*, **10**, 120 (1952).

Peaceman, D. W., and H. H. Rachford, Jr., "The Numerical Solution of Parabolic and Elliptic Differential Equations," *J. Soc. Ind. Appl. Math*, **3**, 28 (1955).

Rogers, M. H., and G. N. Lance, "The Boundary Layer on a Disc of Finite Radius in a Rotating Fluid," *Quart. J. Mech. Appl. Math.*, **17**, 319 (1964).

Rott, N., and W. S. Lewellen, "Boundary Layers and Their Interactions in Rotating Flows," *Progr. Aeronaut. Sci.*, **7**, 111 (1966).

Schlichting, H., Boundary Layer Theory, 4th Edit., McGraw-Hill, N. Y. (1960).

Sparrow, E. M., and J. L. Gregg, "Heat Transfer from a Rotating Disk to Fluids of Any Prandtl Number," *J. Heat Transfer, Trans. ASME, Ser. C.*, **81**, 249 (1959).

Manuscript received November 24, 1971; revision received May 19, 1972; paper accepted May 19, 1972.

Mass Transfer to a Rotating Fluid

Part II. Transport from the Base of an Agitated Cylindrical Tank

Mass transfer to the base of an unbaffled cylindrical tank which is agitated by an axially-mounted impeller is studied experimentally and theoretically. Measured local mass transfer coefficients vary with radial position and fall within theoretical bounds derived for the case of a fluid undergoing solid body rotation above the boundary layer on the base. Average mass transfer coefficients and torque delivered to the base are fitted by consistent theoretical expressions, and an empirical correlation is developed for calculating the average liquid phase mass transfer coefficient.

CLARK K. COLTON and KENNETH A. SMITH

Department of Chemical Engineering
Massachusetts Institute of Technology
Cambridge, Massachusetts 02139

SCOPE

The stirred tank is a convenient geometry for the study of interfacial mass transport and the measurement of membrane transport properties. For example, diffusive permeability is commonly measured in a dialysis cell in which a membrane separates two identical unbaffled cylindrical chambers, each of which is agitated by an axially-mounted impeller placed in close proximity to the membrane surface. A similar arrangement may be employed, sometimes with only one chamber and a supported membrane, for the evaluation of filtration properties.

Assessment of intrinsic membrane properties is complicated by the resistance to mass transfer offered by the concentration boundary layers adjacent to the membrane. Transport of a rapidly permeating solute across a membrane may be wholly or partially rate-controlled by these boundary layers and not by the membrane at all. The usual approach is to minimize the liquid-phase resistances by intense stirring. Some workers have used a Wilson Plot method wherein measurements are made at different stirring speeds and extrapolated to infinite speed. In few instances has the average mass transfer coefficient been measured directly, and never previously in the specific

system of interest here. An additional problem arises in the likely event that the local mass transfer coefficient varies with position. This may lead to serious misinterpretation of data if the boundary layer or membrane phenomena are concentration dependent.

This paper is concerned with a detailed characterization of mass transfer in such a system. The problem is treated theoretically by employing a simplified picture of the flow pattern between the impeller and base. It is assumed that at some distance from the base there exists a core undergoing solid body rotation. Flow in the boundary layer on the base is predominantly radially inward and axially upward. The angular velocity in the core above the boundary layer is treated as an adjustable parameter, and bounding estimates are obtained first, by setting it equal to the impeller angular velocity, and second, by treating the impeller as though it were a rotating disk. Estimates of fluid shear stress at the surface are obtained for laminar and turbulent boundary layers from existing solutions of the fluid dynamic problem. Estimates of mass transfer coefficients for a laminar boundary layer are obtained from a companion paper (Smith and Colton, 1972) which deals with transport from a rotating fluid to finite stationary disk situated on an infinite surface. The effect of a simultaneously developing momentum boundary layer on a finite surface is also considered here. Estimates for a turbulent boundary layer are obtained from a special form of the Chilton-Colburn analogy.

Experimental measurements of average and local mass transfer coefficients are made at various stirrer speeds in one chamber of a batch dialyzer by replacing the membrane with a plate containing a compressed, slightly soluble organic solid. Average values are obtained by following the change in chamber concentration with time, and local coefficients are determined by measuring the depth of solid removed. Measurements of total power dissipated in the chamber and of torque delivered to the stationary base are made in a full scale replica of the device.

CONCLUSIONS AND SIGNIFICANCE

Local mass transfer coefficients fall between the bounds of the theoretical estimates. At low Reynolds numbers, a laminar boundary layer prevails and the surface is nonuniformly accessible. Local coefficients decrease uniformly from the edge of the base, except as modified by the presence of the sidewalls, and become nearly zero at the center (Figure 3). The radial dependence is also present (but to a lesser extent) at Reynolds numbers sufficiently high so that the boundary layer is turbulent (Figure 4). The results demonstrate that the mass transfer correlation is properly scaled if a single characteristic dimension, the radius of the transferring surface, is employed.

Measurements of torque delivered to the base of the tank and of area-averaged mass transfer coefficients are successfully fitted by consistent theoretical expressions. An empirical correlation from which average liquid phase mass transfer coefficients may be estimated is presented for Reynolds numbers ranging from 8×10^3 to 8×10^4.

Membrane transport properties are often evaluated in a simple system comprised of a membrane clamped between two identical unbaffled stirred chambers. Evaluation of these properties is sometimes limited by knowledge of mass transfer in the concentration boundary layers adjacent to the membrane. Helfferich (1956), for example, has shown that measurements with ion exchange membranes in bi-ionic cells are particularly prone to boundary layer influences. With regard to the study of rapidly permeating solutes in natural biological membranes, Dainty (1963) has cast doubt on the validity of available data and has shown that the experimental evidence for the existence of water-filled pores in cell membranes is likely an artifact caused by failure to evaluate the liquid phase mass transfer resistance. The latter may also be the controlling resistance in the study of highly permeable synthetic membranes for hemodialysis, where intrinsic membrane resistances equivalent to a stagnant film of water as thin as about 20 μm have been reported (La Conti et al., 1971). Concentration boundary layer effects are also known to have a controlling influence on the ultrafiltration of solutions of macromolecules (Blatt et al., 1970; Goldsmith, 1971).

The system of interest here consists of two axially-mounted turbine or paddle impellers, each placed in close proximity to one face of the membrane. The problem of accounting for liquid phase transport resistances in such devices has been handled by a variety of techniques, including minimization of these influences by operation above an empirically determined impeller speed (Marshall and Storrow, 1951; Lane and Riggle, 1958) in the manner suggested by Stokes (1950), estimation of a hypothetical stagnant diffusion film thickness which is assumed to be independent of solute properties (Gregor and Peterson, 1959; Mackay and Meares, 1959; Helfferich, 1962; Ginzberg and Katchalsky, 1963), and extrapolation of data to infinite stirrer speed by use of a Wilson Plot (Wilson, 1915; von Kiss and Urmanczy, 1935; Leonard and Bluemle, 1962; Kaufmann and Leonard, 1968a).

Scattergood and Lightfoot (1968) made direct measurements of the average mass transfer coefficient over a range of stirrer speeds using electrochemical techniques by replacing the membrane with an electrode, as did Holmes et al. (1963). Neither work is directly applicable here because the former study employed a propeller (Scattergood, 1965) and the latter was carried out in a diaphragm diffusion cell in which a magnetized stirring bar was rotated in a plane perpendicular to the diaphragm surface. Kaufmann and Leonard (1968b) used their Wilson plot results obtained in the system of interest here to determine the dependence of the average mass transfer coefficient on Schmidt and Reynolds numbers. Johnson and Huang (1956) studied mass transfer to annular rings of organic solids at the bottom of unbaffled and baffled stirred tanks and noted a dependence of the mass transfer coefficient on radial position; their analysis of the Schmidt number dependence was later questioned (Marangozis and Johnson, 1962). Marangozis and Johnson (1961) used a similar technique with only baffled tanks. These authors later presented a correlation (Marangozis and Johnson, 1962)

based upon data for suspended solids in unbaffled tanks and, by comparison with data from the bottom of baffled tanks, they implied that it was valid for the bottom of unbaffled tanks as well. Calderbank and Moo-Young (1961) developed a correlation using power input per unit volume which was derived from the theory of locally isotropic turbulence (Kolmogoroff, 1941). Based largely upon data for dispersed particles, they claimed it to be valid for fixed surfaces in tanks of arbitrary configuration.

Thus studies to date have been limited in scope and largely empirical in nature. Spatially-dependent local mass transfer coefficients have been observed but not studied in any depth; hence their potential consequences have gone unappreciated. This paper has two objectives: first, to present a detailed experimental study of mass transport from the base of an agitated cylindrical tank; and second, to compare these results with theoretical models describing the transport process. This comparison is facilitated by knowledge of the torque exerted by the fluid at the active surface, experimental measurements of which are also reported. However, the detailed flow field in a stirred tank is of such complexity as to preclude an exact analysis, and the theoretical models proposed here are concerned with a description of the quantitatively important features rather than with the fine structure. Direct utilization of some of the results described in this paper for the evaluation of intrinsic membrane properties from a single experimental measurement has been described previously (Smith et al., 1968; Colton et al., 1971).

THEORETICAL DESCRIPTION

Consider an axially-mounted turbine or paddle impeller situated in a cylindrical tank with a flat bottom (Figure 1). Rotation of the impeller with an angular velocity ω sets the fluid in the tank into rotary motion. The following simplified but conceptually useful picture of the gross flow is assumed. Thin momentum boundary layers form on the impeller (qualitatively regarded as a spinning disk), on the stationary base, and on the cylindrical sidewall. The fluid core outside the boundary layers rotates as a solid body with angular velocity $\gamma\omega$, $0 < \gamma \leq 1.0$. All radial flow occurs within the boundary layers; fluid flows radially outward in the boundary layer on the impeller and radially inward on the stationary base. This leads to a spiral-like flow pattern on the stationary base, as was observed in this study (see Results and Discussion). Continuity suggests an axial upflow (except near the sidewall) over the entire region. This description is consistent with the qualitative observations of Lehmkuhl and Hudson (1971).

It is desirable to relate the angular velocity of the inviscid core to a more accessible parameter, the impeller velocity. This can be readily accomplished for two limiting cases which seem to provide upper and lower bounds to the true physical situation. First, it is assumed that the fluid beyond the boundary layers rotates with the same angular velocity as the impeller ($\gamma = 1.0$). That is to say, the boundary layer on the impeller vanishes and the boundary layer on the stationary base sees a fluid undergoing solid body rotation with angular velocity ω. In the second case, the impeller is thought to be replaced by a disk of equivalent radius, and the problem becomes formally identical to that of a disk rotating in a right-cylindrical enclosure. The fluid dynamics of the latter situation has been studied in some detail (Schultz-Grunow, 1935; Ippen, 1946; Pantell, 1950; Soo, 1958; Daily and Nece, 1960; Dorfman, 1963; Tomlan and Hudson, 1971; Lehmkuhl and Hudson, 1971), and the available approximate solutions provides a means for estimating γ. Schultz-Grunow analyzed the two boundary layer problem for both laminar and turbulent regimes using the von Karman momentum integral technique and the 1/7th-power velocity distribution for the latter case. His solution provides an estimate of the torque on the disk and on the base. By imposing the compatibility condition that these two quantities be equal, it is possible to solve for γ in terms of the geometric ratio b/a. Although the equations are cumbersome, the calculation is straightforward, and details are given elsewhere (Colton, 1969). For the ratio employed in this study ($b/a = 1.11$), we obtain $\gamma = 0.44$ and 0.48 for laminar and turbulent boundary layers respectively. Daily and Nece (1960) included the influence of the sidewall and focused on the effect of the ratio s/a with a more approximate analysis. With the value employed here ($s/a = 0.112$), the estimate of γ would be slightly lower than that cited above.

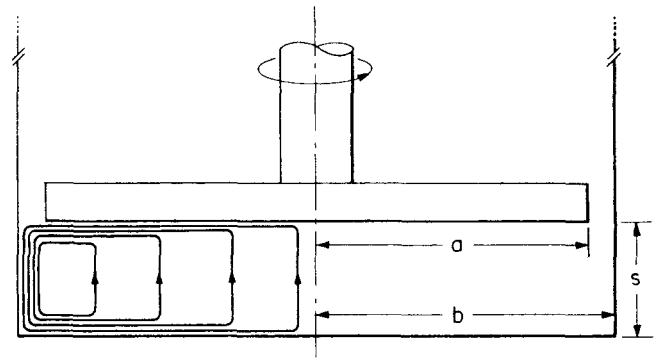

Fig. 1. Proposed flow patterns near base of stirred tank.

Theoretical relationships are derived for the mass transfer coefficient and the turning moment on the stationary base. While of less direct interest, the latter quantity is included because it provides an internal consistency check in comparing the theoretical expressions with experimental data, that is, the same value of γ should fit both mass transfer and torque measurements. For a laminar boundary layer, the problem is treated as that of a fluid which undergoes solid body rotation at a large distance from an infinite stationary surface with mass transfer to or from a finite disk on that surface. The momentum boundary layer equations for this problem were solved by Bödewadt (1940), and the mass transfer problem is considered in detail in a companion paper (Smith and Colton, 1972). For a turbulent boundary layer, the expressions obtained by Schultz-Grunow (1935) for the wall shear stress components are employed in conjunction with a form of the Chilton-Colburn (1934) momentum-mass transport analogy for turbulent flow.

Laminar Boundary Layer

The turning moment on a stationary disk of radius b is given by

$$M = 2\pi \int_0^b \tau_{z\phi}\, r^2 dr = \frac{1}{2}\rho\omega^2 b^5 C_M \qquad (1)$$

If $\tau_{z\phi}$ is taken from the Bödewadt (1940) solution for the velocity field, then

$$C_M = 2.43\, \gamma^{3/2}\, Re^{-1/2} \qquad (2)$$

From the results of Smith and Colton (1972), the local mass transfer coefficient for high Schmidt number may be expressed in the form

$$St\ Sc^{2/3}\ Re^{1/2} = \gamma^{1/2}\ f(x) \tag{3}$$

where $f(x)$ is determined by numerical solution of the complete two dimensional convective diffusion equation. The overall transport process is effectively dominated by the leading (circular) edge where the concentration boundary layer initially develops, for which region the solution is

$$St\ Sc^{2/3}\ Re^{1/2} = 0.528\ \gamma^{1/2}\left[\ln\left(\frac{1}{x}\right)\right]^{-1/3}$$

$$\cong 0.528\ \gamma^{1/2}\ (1-x)^{-1/3} \tag{4}$$

As Schmidt number increases towards infinity, the area-averaged mass transfer coefficient tends towards the asymptotic expression

$$\overline{St}\ Sc^{2/3}\ Re^{1/2} = 0.768\ \gamma^{1/2} \tag{5}$$

Use of the similarity solution of Bödewadt for the velocity field above the base of a stirred tank entails two potentially critical deficiencies. First, the base is not infinite and would be better represented as a finite disk. Secondly, the boundary layer on the cylindrical sidewall is completely neglected. The latter problem is not readily amenable to analytic treatment because of lack of quantitative knowledge of its influence on the velocity field, and judgement as to the appropriateness of neglecting this feature in the mass transfer analysis rests with a comparison with experimental data. The former problem, however, is treated below by carrying out an analysis for the leading edge where both momentum and concentration boundary layers are developing. To facilitate comparison, the coordinate system and notation of both Rogers and Lance (1964) and Smith and Colton (1972) will be adhered to where possible.

The radial and axial velocity components are given by Rogers and Lance (1964) as

$$V_r = -\frac{1}{r}\frac{\partial \Psi}{\partial z} \tag{6}$$

$$V_z = \frac{1}{r}\frac{\partial \Psi}{\partial r} \tag{7}$$

where

$$\Psi = b^2(\gamma\omega\nu)^{1/2}\ (1-x)^{3/4} \sum_{n=0}^{\infty} \psi_n\ (\eta)\ (1-x)^n \tag{8}$$

and

$$\eta = z\left(\frac{\gamma\omega}{\nu}\right)^{1/2}(1-x)^{-1/4} \tag{9}$$

If one notes that $1/r = (1/b)\sum_{m=0}^{\infty}(1-x)^m$, the result may be expressed as

$$V_r = -(\gamma\omega b)\sum_{n=0}^{\infty}\sum_{m=0}^{\infty}[\psi_n'\ (1-x)^{n+m+1/2}] \tag{10}$$

and

$$V_z = -(\gamma\omega\nu)^{1/2}\sum_{n=0}^{\infty}\sum_{m=0}^{\infty}\left[-\frac{1}{4}\eta\ \psi_n' + \left(n+\frac{3}{4}\right)\psi_n\right](1-x)^{m+n-1/4} \tag{11}$$

Near the leading edge where, for high Schmidt number, the developing concentration boundary layer is imbedded well within the momentum boundary layer, we may approximate $\psi_n(\eta)$ and $\psi_n'(\eta)$ by the first nonzero terms in their respective Maclaurin series expansions, whence

$$V_r \cong -(\gamma\omega b)\eta\sum_{n=0}^{\infty}\sum_{m=0}^{\infty}[\psi_n''(0)\ (1-x)^{n+m+1/2}] \tag{12}$$

and

$$V_z \cong -\frac{1}{2}(\gamma\omega\nu)^{1/2}\ \eta^2\sum_{n=0}^{\infty}\sum_{m=0}^{\infty}\left[\left(n+\frac{1}{4}\right)\psi_n''(0)\ (1-x)^{m+n-1/4}\right] \tag{13}$$

since $\psi_n'(0) = 0$, all n. From Rogers and Lance (1964), $\psi_n''(0) = 1.0681$, -1.9855, and 0.7301 for $n = 0$, 1, and 2, respectively. Note that, near the surface, the functional dependence of the velocity components on z is precisely the same as that found from the Bödewadt solution (Smith and Colton, 1972), the sole difference being the additional radial dependence, as shown in Figure 2. The axial inflow near the leading edge is qualitatively consistent with the physical requirements of a stirred tank (Figure 1).

Within the boundary layer context, radial diffusion may be neglected in comparison to axial diffusion. If we further restrict attention to $(1-x) << 1$, then all terms in the radial series expansion except the first $(m = n = 0)$ may be neglected. A treatment similar to the leading edge solution of Smith and Colton (1972) can then be executed with no essential difference except that axial convection is retained, and the convective diffusion equation becomes

$$\frac{d^2\theta}{d\eta^2} + \frac{3}{8}\,Sc\ \psi_0''(0)\ \eta^2\frac{d\theta}{d\eta} = 0 \tag{14}$$

Equation (14) is of the same form as Equation (22) in Smith and Colton (1972) and, with identical boundary conditions, leads to a similar solution. The dimensionless mass transfer coefficient is found to be

$$St\ Sc^{2/3}\ Re^{1/2} = \frac{\gamma^{1/2}}{\Gamma\left(\frac{4}{3}\right)}\left[\frac{\psi_0''(0)}{8}\right]^{1/3}[1-x]^{-1/4}$$

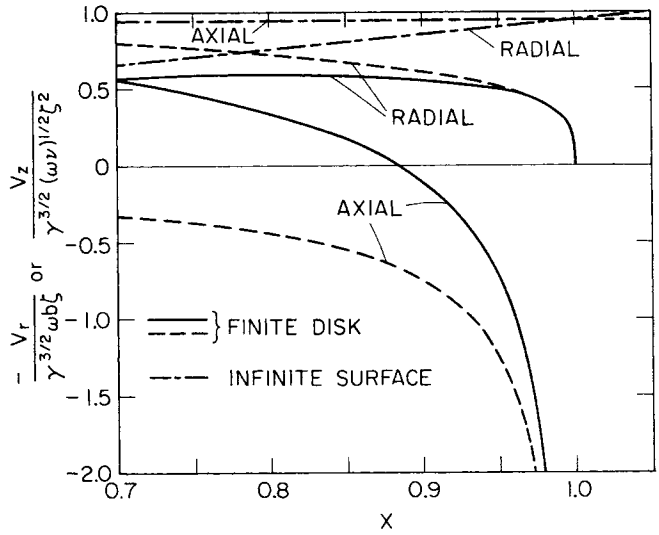

Fig. 2. Radial and axial velocity components near the wall ($\eta << 1$) at the leading edge of a finite stationary disk in a rotating fluid. Solid curves-three terms in series; dotted curves-first term only. Intermittently dotted curves are comparable profiles for solid body rotation above an infinite stationary surface. Note that $\zeta = \eta(1-x)^{1/4}$.

$$= 0.572\ \gamma^{1/2}[1 - x]^{-1/4} \qquad (15)$$

Consequently, the leading edge result for a finite disk is remarkably similar to Equation (4) and demonstrates the efficacy of employing the Bödewadt velocity profiles. From Figure 2, it is evident that a first-order representation of the axial velocity provides an upper bound on the associated axial convection for the leading edge. However, even if axial convection is deleted entirely, the sole effect is to change the coefficient in Equation (15) to 0.500.

Similar behavior is found for the frictional shear stress. From Rogers and Lance (1964), use of the finite disk profiles over the outer half of the disk (and the similarity solution over the remainder) leads to

$$C_M = 2.25\ \gamma^{3/2}\ Re^{-1/2} \qquad (16)$$

which is only modestly different from Equation (2).

Turbulent Boundary Layer

Schultz-Grunow (1935) employed the von Karman momentum integral technique with a power law distribution of velocity components in the boundary layer

$$V_\phi = \gamma\omega r(z/\delta)^{1/7} \qquad (17)$$

$$V_r = \alpha\gamma\omega r(z/\delta)^{1/7}\left(1 - \frac{z}{\delta}\right) \qquad (18)$$

Consequently, a velocity scale U appropriate for the flow very close to the surface is given by

$$\lim_{z\to 0} \sqrt{V_r^2 + V_\phi^2} \to \gamma\omega r\sqrt{(1+\alpha^2)}\left(\frac{z}{\delta}\right)^{1/7} = U(z/\delta)^{1/7} \qquad (19)$$

and it was assumed that the Blasius (1915) semi-empirical shear stress correlation remains valid if expressed in terms of U:

$$\tau_0 = \sqrt{\tau_{zr}^2(0) + \tau_{z\phi}^2(0)} = 0.0225\ \rho\ U^2\left(\frac{\nu}{U\delta}\right)^{1/4} \qquad (20)$$

Furthermore, it was assumed that, as for the laminar case

$$\frac{\tau_{zr}(0)}{\tau_{z\phi}(0)} = \lim_{z\to 0}\left(\frac{V_r}{V_\phi}\right) = \alpha \qquad (21)$$

Closure was then achieved by utilizing the integral equations

$$\frac{\tau_{zr}(0)}{\rho} = -\frac{1}{r}\int_0^\delta [(\gamma\omega r)^2 - V_\phi^2]\,dz - \frac{1}{r}\frac{d}{dr}\left[r\int_0^\delta V_r^2\,dz\right] \qquad (22)$$

and

$$\frac{\tau_{z\phi}(0)}{\rho} = -\int_0^\delta \frac{1}{r^2}\frac{\partial}{\partial r}(r^2 V_r V_\phi)\,dz + \gamma\omega\frac{d}{dr}\int_0^\delta rV_r\,dz \qquad (23)$$

In this regard, it may be noted that the forms given by Dorfmann (1963) are incorrect. Schultz-Grunow (1935) obtained a solution to the foregoing by assuming $(\alpha^2 + 1)^{3/8} \cong 1$, which limits validity to roughly the outer 1/3 of the base. His results may be expressed in the form

$$\alpha = (1-x)^{1/2}\frac{g_1(x)}{g_2^4(x)} \qquad (24)$$

$$\frac{\delta}{b} = \frac{(1-x)}{\delta^{1/5}\,Re^{1/5}}\,g_2^4(1-x) \qquad (25)$$

where

$$g_1(x) = 0.4254 - 1.894(1-x) + 4.47(1-x)^2 - 6.945(1-x)^3 + 6.78(1-x)^4 \qquad (26)$$

$$g_2(x) = 0.8554 - 1.063(1-x) + 0.814(1-x)^2 + 3.397(1-x)^4 \qquad (27)$$

If Equations (20) through (21) and (23) through (27) are combined with Equation (1) and an integration performed, there results

$$C_M = 0.1074\ \gamma^{9/5}\ Re^{-1/5} \qquad (28)$$

(Note that the constant in Equation (28) was originally given by Schultz-Grunow as 0.1038).

The Chilton-Colburn analogy may be expressed as

$$\frac{k}{U}\,Sc^{2/3} = \frac{\tau_0}{\rho U^2} \qquad (29)$$

where, following the approach of Eckert and Jackson (1951), the characteristic velocity is again taken to be U. With the above results Equation (29) leads to

$$St\ Sc^{2/3}\ Re^{1/5} = 0.02225\ \gamma^{4/5}\frac{(1+\alpha^2)^{3/8}\,x^{3/4}}{(1-x)^{1/10}\,g_2(x)} \qquad (30)$$

and the area-averaged Stanton number is

$$\overline{St}\ Sc^{2/3}\ Re^{1/5} = 0.0323\ \gamma^{4/5} \qquad (31)$$

EXPERIMENT

Measurements of mass transfer coefficients were carried out in one chamber of a batch dialyzer with the membrane replaced by an aluminum plate containing an insert of compressed benzoic acid. The benzoic acid was warmed to a temperature just below its melting point and compressed, then cooled, sanded flat, and washed. Dimensions of the active transfer surface on the various plates employed are given in Table 1. Plates 2, 3, and 4 were annular rings, and plates 1 and 5 were disks, the latter covering the entire chamber diameter.

The chamber was 6.304 cm in diameter and 7.62 cm long and was jacketed for temperature control (± 0.1°C). An axially-mounted, four-blade paddle impeller, with blades 5.68 cm in diameter, 0.635 cm wide, and 0.1588 cm thick, was positioned 0.3175 cm from the base (unless otherwise indicated). All experiments were run at 25°C. Impeller speeds were varied from about 70 to 700 rev./min.

An aqueous solution of 0.002 M benzoic acid was initially charged to the chamber and the desired impeller speed maintained constant to within ± 1 rev./min. Concentration in the chamber was monitored conductiometrically and recorded. The data was plotted as suggested by

$$\ln\left[\frac{c_w - c}{c_w - c_0}\right] = -\frac{\overline{k}\,A\,t}{V_c} \qquad (32)$$

Table 1. Dimensions of Cast Benzoic Acid

Plate	Inside diam. ($2r_2$), cm	Outside diam. ($2r_1$), cm	Mass transfer area, cm²
1	0	1.40	1.53
2	1.36	2.44	3.23
3	3.40	4.21	4.81
4	5.30	5.74	3.85
5	0	6.30	31.21

and the average mass transfer coefficient was calculated accordingly. It was assumed that a quasi steady state prevailed in the concentration field near the surface, thus permitting a comparison with the steady state theoretical models. The concentration at the wall c_w was taken to be the saturation concentration 0.0280 M (Seidell, 1940). Values of the molecular diffusion coefficient were taken from the results of Chang (1949) and evaluated at the time-mean of the average of wall and bulk concentrations.

Local mass transfer coefficients were determined by measuring the depth of benzoic acid dissolved (referred to the originally flat surface), using a displacement transducer (Indi-Ac, Cleveland Instr. Co., Model A-215-R) sensitive to about 10^{-6} cm. Two radial traverses were made across the entire diameter in perpendicular directions and the results averaged. The solid benzoic acid was assumed to be of uniform density and the local mass transfer coefficient determined from

$$\frac{k}{\bar{k}} = \frac{\epsilon}{\left(2\int_{r_2}^{r_1} \epsilon r dr\right)/(r_1^2 - r_2^2)} \tag{33}$$

where ϵ is the radially-dependent depth of benzoic acid dissolved and the denominator on the right of Equation (33) was obtained by numerically integrating the experimental data. After a typical run, the average displacement of the surface was of order 10^{-2} cm on plate 5, thus ensuring no significant alteration in the velocity field near the surface over the course of a run. Unfortunately this was not necessarily the case with the other plates, particularly plate 1, because of the greatly reduced transfer area.

Torque measurements were made at room temperature in a full-scale replica of the dialyzer chamber with the impeller shaft entering through a narrow neck at the top. The chamber bottom, which rested on a calibrated flexural pivot, was 0.051 cm smaller in diameter than the cylindrical sidewall and could rotate freely while the latter was rigidly held, thereby permitting measurement of the torque applied to the flat interface alone. A mercury seal at the bottom prevented pumping of liquid out of the chamber. Total power dissipated in the chamber was measured by rigidly connecting the bottom and sidewall with an O-ring and leaving the entire vessel free to rotate.

Flow visualization studies were carried out in a single dialyzer chamber with the membrane replaced by a transparent Lucite endplate. An optically thick suspension (> 1% by volume) of reflective, microscopic anisotropic particles (Mearlmaid AQ, Mearl Corp., N.Y.) was placed in the chamber. Alignment of the particles in a shear field permitted direct visualization of flow patterns within less than 0.05 cm of the endplate surface.

Additional details of the equipment and procedure have been described elsewhere (Smith et al., 1968; Colton, 1969).

RESULTS AND DISCUSSION

The flow patterns observed in the flow visualization studies displayed spiral-like behavior within the boundary layer on the transparent endplate. These patterns were qualitatively similar to those expected for solid body rotation above the stationary base and, in fact, served as an initial clue to the theoretical models developed in this paper.

The local mass transfer coefficients measured with plate 5 are shown in Figures 3 and 4 and compared with theoretically predicted estimates. Figure 3 contains data for $Re < 3.2 \times 10^4$ plotted in the manner suggested by the laminar boundary layer model, Equation (3). The curves shown in Figure 3 were calculated for $Sc = 850$ as described by Smith and Colton (1972). The bulk of the data lies between the bounding limits of free stream rotation with the impeller on the one hand and replacement of the impeller by a rotating disk on the other. The sole exception to this generalization is the region immediately adjacent to the cylindrical sidewall. The decrease in the mass transfer coefficient which occurs there is clearly due to the sidewall boundary layer. The maximum occurs in the range of $x = 0.97$ to 0.94, corresponding to about 1 to 2 mm from the wall, a distance roughly comparable to

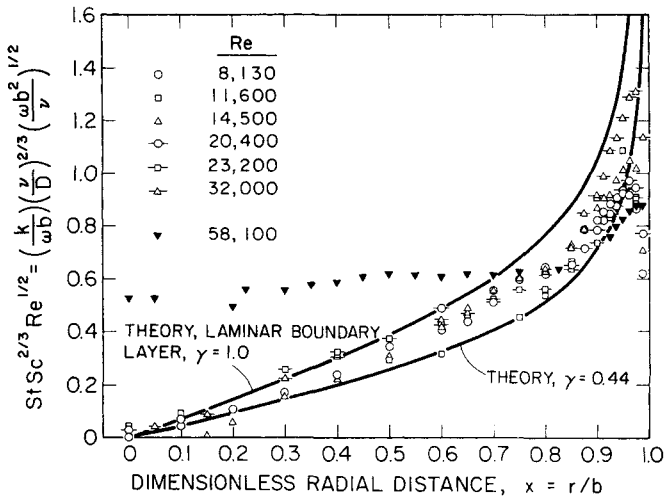

Fig. 3. Dependence of dimensionless local mass transfer coefficients on dimensionless radial position. Lower Reynolds number data from plate 5.

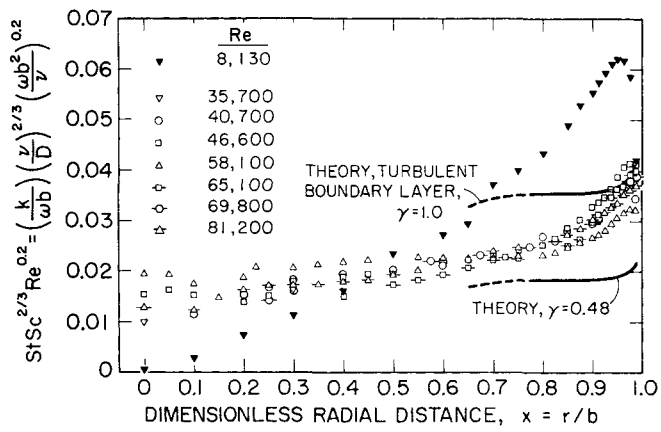

Fig. 4. Dependence of dimensionless local mass transfer coefficients on dimensionless radial position. Higher Reynolds number data from plate 5.

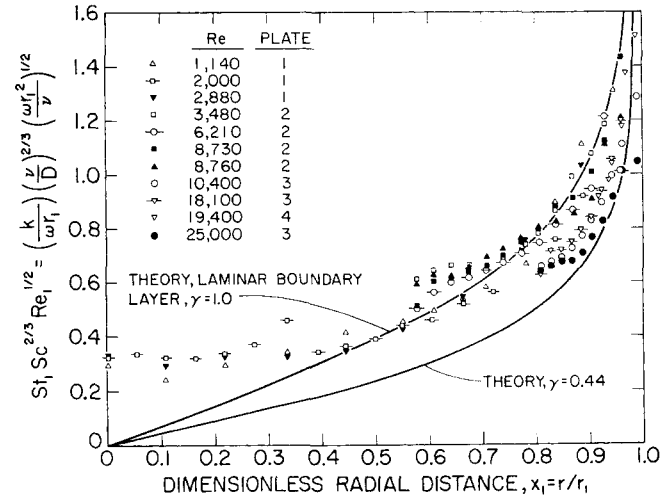

Fig. 5. Local mass transfer coefficients obtained with plates 1 through 4. Note that characteristic length is taken as r_1.

the momentum boundary layer thickness on the stationary base. Over the remainder of the transport surface, the local mass transfer coefficient decreases continuously, as the distance from the sidewall increases, to nearly zero at the center, in remarkable agreement with the radial dependence predicted for Bödewadt flow over the base.

Also plotted in Figure 3 is a set of data for $Re = 5.8 \times 10^4$ which displays a markedly different dependence on radial position. This is examined further in Figure 4 which contains data for $Re > 3.5 \times 10^4$ plotted as suggested by the turbulent boundary layer model, Equation (30). The data again falls, for the most part, between the bounding limits of the theoretical solution. The latter is limited in validity to the outer 1/3 of the transfer surface, and erroneously predicts $St = 0$ at $x = 0$, whereas the data indicate that the local mass transfer coefficient becomes constant, or decreases only slightly, towards the center of the base. This is in marked contrast to the behavior at lower Reynolds number, for which a set of data is again plotted for comparison.

In the region near the sidewall, a sharp decrease in mass transfer coefficient is not observed at the higher Reynolds numbers, and the weak maximum occurs much closer to the wall. This is consistent with a decreased influence of the thinner sidewall boundary layer. Taken together, Figures 3 and 4 suggest a transition from a laminar to a turbulent boundary layer at $Re \simeq 3.2 \times 10^4$ over most of the surface of the base. The leading edge behavior in Figure 4 shows a greater radial dependence than predicted by the turbulent boundary layer model. While this dependence is clearly less than predicted for a laminar boundary layer, it may suggest some laminar-like behavior in the velocity field near the leading edge.

Local mass transfer coefficients obtained with plates 1 through 4 are shown in Figure 5 and compared with the theoretical laminar boundary layer model. In the leading edge region, the data fall between the theoretical bounds, and a maximum in the local mass transfer coefficient is not apparent because of the absence of an adjacent sidewall. Away from the leading edge, the data from all runs show a consistent departure from the predicted radial dependence. A distinguishing feature of these runs, in comparison to those with plate 5 (Figure 3), is that the benzoic acid was removed to a much greater depth (since the runs were longer) to compensate for the greatly reduced transfer area. It is suggested that this affected the local velocity field so as to bring about the observed behavior. Despite this anomaly and the lack of absolute agreement between runs with different plates, the data suggest that the mass transfer coefficients are correctly scaled by using r_1, the outer radius of the transfer surface (b in the case of plate 5), as the characteristic length in all dimensionless groups rather than the impeller or tank dimension as is conventionally employed. As a consequence, the local mass transfer coefficient is dependent only on the dimensionless radial coordinate and is independent of the disk radius (as is the average mass transfer coefficient), all other parameters being held constant.

The local mass transfer coefficient results in Figures 3, 4, and 5 clearly demonstrate that the true value of γ in the inviscid core lies within the prescribed bounds, although experimental scatter and the presence of the sidewall prevents its precise evaluation. These results also suggest that the dependence of mass transfer coefficient on Reynolds number is adequately represented by the theoretical relations. With regard to measurements of the torque on the stationary base and the area-averaged mass transfer coefficient, it is convenient to treat γ as an

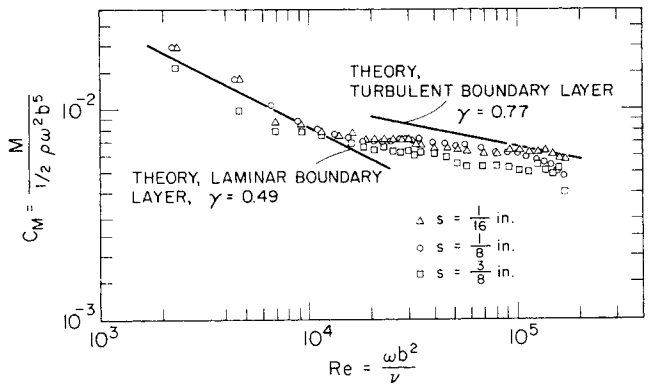

Fig. 6. Moment coefficient, from torque applied to stationary base, as a function of Reynolds number and various axial gap ratios. Theoretical lines are plotted with $\gamma = 0.49$ and 0.77 for laminar and turbulent boundary layers, respectively.

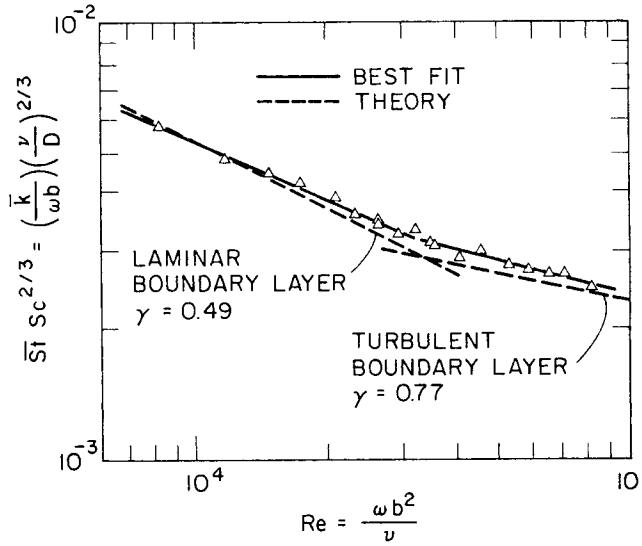

Fig. 7. Dimensionless correlation of area-averaged mass transfer coefficients.

adjustable parameter to be determined empirically, with the proviso that the same value of γ must fit both the torque and the mass transfer results. Such a comparison is shown in Figures 6 and 7. The theoretical lines correspond to Equations (16) and (28) for the dimensionless moment coefficient and to Equations (5) and (31) for the average mass transfer coefficient. It is found that a fit between theory and data is obtained with γ set equal to 0.49 and 0.77 for laminar and turbulent boundary layers, respectively. The laminar value is close to the predicted value of γ. The turbulent value is significantly higher, but not surprisingly so in view of the limited region of validity of the model. Of more importance is the fact that a unique value of γ fits both sets of data reasonably well within each flow regime.

The results in Figure 6 show a very modest influence of the dimensionless axial gap so long as the impeller is in relatively close proximity to the base. The data show laminar behavior up to a Reynolds number of about 1.5×10^4. This is followed by a transition region, and by turbulent behavior above a Reynolds number of about 3×10^4. The torque delivered to the base typically represented about one-tenth of that delivered to the entire vessel.

The average mass transfer coefficient data in Figure 7

are consistent with a transition from a laminar to turbulent boundary layer at a Reynolds number of about 3×10^4. An empirical fit to the data, using a weighted least squares analysis, gives

$$8 \times 10^3 < Re \leq 3.2 \times 10^4 \quad \overline{St}\, Sc^{2/3} = 0.285\, Re^{-0.433} \tag{34}$$

$$8.2 \times 10^4 > Re \geq 3.2 \times 10^4 \quad \overline{St}\, Sc^{2/3} = 0.0443\, Re^{-0.254} \tag{35}$$

The Schmidt number dependence was not tested in this study but is reasonable in view of the results of Kaufmann and Leonard (1968b) in a similar system and its firm theoretical foundation for both flow regimes.

It is useful to compare these results with other empirical correlations which have appeared in the literature. Kaufmann and Leonard (1968a) estimated mass transfer coefficients from their Wilson plot data over a wide range of Schmidt and Reynolds numbers. They obtained

$$\frac{\overline{k}d}{D} = 0.105\, Sc^{0.32} \left(\frac{\omega d^2}{\nu}\right)^{0.68} \tag{36}$$

Conversion to the characteristic dimension (b) employed here at a Schmidt number of 850 leads to

$$\overline{St}\, Sc^{2/3} = 0.121\, Re^{-0.32} \tag{37}$$

Equation (37) is plotted in Figure 8, along with Equations (34) and (35), and appears to predict mass transfer coefficients higher than this study by about 25%. However, the Kaufmann-Leonard correlation was obtained with permeable membranes and with a slightly different geometry. Means for making an approximate correction for these factors have been described (Smith et al., 1968). The results of Smith and Colton (1972) are employed to account for the influence of a permeable wall (rather than one of uniform concentration); this correction is relatively large, about 25%. The theoretical results of Schultz-Grunow (1935) and Daily and Nece (1960) for a laminar boundary layer are employed to estimate the relative change in γ as a function of the geometric ratios b/a and s/a; these corrections are smaller, about 5%. The resulting correlation, in a sense normalized to the conditions of this study, is given by

$$\overline{St}\, Sc^{2/3} = 0.0880\, Re^{-0.32} \tag{38}$$

and is plotted in Figure 8 as a dotted line, along with the data, similarly treated, of Mackay and Meares (1959). The agreement with the results of this study is excellent.

Two other correlations have appeared which purport to apply to transport to fixed surfaces in unbaffled stirred vessels but which are based largely on data obtained with suspended particles. Calderbank and Moo-Young (1961) found for agitation under turbulent conditions

$$\overline{k}\, Sc^{2/3} = 0.13 \left[\frac{P_\mu}{V_c \rho^2}\right]^{1/4} \tag{39}$$

This may be rearranged to yield

$$\overline{St}\, Sc^{2/3} = 0.0216 \left[\frac{N_p}{Re}\left(\frac{b}{h}\right)\right]^{1/4} \tag{40}$$

For the power number, Phipps (1967) found $N_p \simeq 2.64\, Re^{-0.2}$ for $Re \gtrsim 4 \times 10^4$ in the replica used in this study, in which case Equation (40) becomes

$$\overline{St}\, Sc^{2/3} = 0.0263\, Re^{-0.3} \tag{41}$$

Marangozis and Johnson (1962) obtained for unbaffled agitated tanks

$$\frac{\overline{k}L}{D} = 0.635\, Sc^{1/3} \left(\frac{nd^2}{\nu}\right)^{0.70} \tag{42}$$

which becomes, for the present system,

$$\overline{St}\, Sc^{2/3} = 0.200\, Re^{-0.3} \tag{43}$$

Equations (41) and (43) are plotted in Figure 8. Both are clearly inappropriate to the system of interest here. Moreover, Equation (39) is based on the concept that the local mass transfer coefficient is everywhere uniform, an assumption not borne out by the data in Figure 4.

By the same token, extrapolation of the results obtained in this study by the methods referred to above so as to account for marked changes in the geometrical ratios s/a and b/a should be done with caution. For example, Lehmkuhl and Hudson (1971) observed no change in flow pattern as b/a changed from nearly unity to 1.25. However, at $b/a \simeq 2.3$ a shear layer formed producing a major qualitative change in the gross flow behavior.

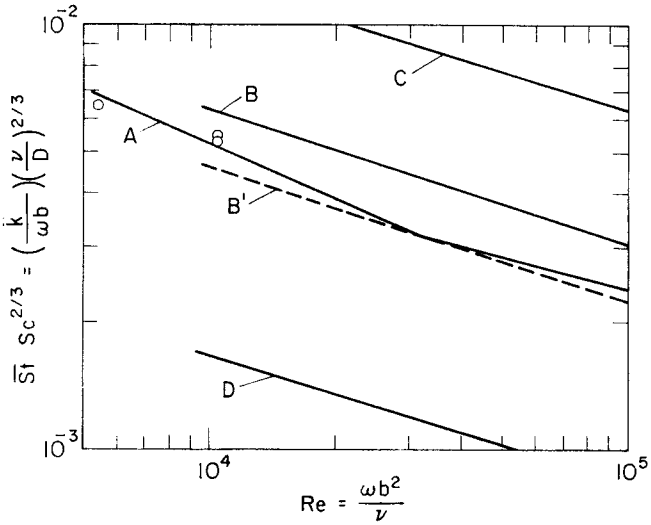

Fig. 8. Comparison of empirical mass transfer correlations. Dotted line is "corrected" correlation as described in text. A—this study; B, B'—Kaufmann and Leonard (1968b); C—Marangozis and Johnson (1962); D—Calderbank and Moo-Young (1961); o—Mackay and Meares (1959).

CONCLUSIONS

With regard to the measurement of membrane permeability, the results presented permit estimation of the area-averaged mass transfer coefficient in the liquid phase. The large variation in the local mass transfer coefficient with relative radial position for a laminar boundary layer, and to a lesser extent for a turbulent boundary layer, has not heretofore been appreciated. Under conditions where the liquid phase constitutes a sizeable fraction of the total mass transfer resistance, and the membrane (or boundary layer) phenomenon is concentration dependent, quantitative conclusions drawn from experimental measurements must give due regard to the nonuniform accessibility of the surface. In such instances, operation with a turbulent boundary layer, if compatible with membrane strength, serves to lessen the problem because of the relatively more constant local mass transfer coefficient.

ACKNOWLEDGMENTS

This study was supported in part by Contract PH 43-66-491 from the National Institute of Arthritis and Metabolic Diseases, NIH, USPHS, and by an NIH Predoctoral Fellowship to C. K. Colton.

NOTATION

A = mass transfer area
b = radius of tank
c = concentration
C_M = dimensionless moment coefficient, $M \Big/ \left(\frac{1}{2}\rho\omega^2 b^5\right)$
d = impeller diameter
D = molecular diffusion coefficient
f = function of x, defined by Equation (3)
g_1, g_2 = functions of x, defined by Equations (26) and (27), respectively
h = height of tank
k = local mass transfer coefficient
$\overline{k}$ = area-averaged mass transfer coefficient
L = diameter of tank
M = torque exerted on base of tank
m = indexing parameter
N_p = power number, $P/n^3 d^5 \rho$
n = indexing parameter; impeller rotational speed
P = power input to tank
r = radial coordinate
r_1, r_2 = outer and inner radius, respectively, of mass transfer surface
Re = Reynolds number, $\omega b^2/\nu$; $Re_1 = \omega r_1^2/\nu$
Sc = Schmidt number, ν/D
St = Stanton number, $k/\omega b$; $St_1 = k/\omega r_1$
$\overline{St}$ = area-averaged Stanton number, $\overline{k}/\omega b$
U = characteristic velocity scale, $\gamma\omega r\sqrt{1+\alpha^2}$
V = velocity
V_c = volume of chamber
x = dimensionless radial coordinate, r/b
z = axial coordinate

Greek Letters

α = dimensionless velocity scaling parameter, defined by Equation (18); see also Equation (24)
$\Gamma(a)$ = gamma function
γ = dimensionless ratio of angular velocity in core above stationary base to impeller angular velocity
δ = momentum boundary layer thickness
ϵ = depth of benzoic acid dissolved
ζ = dimensionless axial coordinate, $z(\gamma\omega/\nu)^{1/2}$
η = dimensionless similarity variable, defined by Equation (9)
θ = dimensionless concentration, $(c - c_\infty)/(c_w - c_\infty)$
μ = viscosity
ν = kinematic viscosity
ρ = density
τ = shear stress
Ψ = stream function
ψ = function of η, defined by Equation (8)
ω = impeller angular velocity, $2\pi n$

Subscripts

o = resultant value at wall; initial value
r = radial
w = wall
z = axial
ϕ = circumferential
∞ = bulk solution

LITERATURE CITED

Blatt, W. F., et al., "Solute Polarization and Cake Formation in Membrane Ultrafiltration:Causes, Consequences and Control Techniques," in J. E. Flinn (ed.), Membrane Science and Technology, Plenum Press, New York, 1970.

Bödewadt, V. T., "Die Drehströmung über festem Grunde," Z. *Angew. Math. Mech.*, **20**, 241 (1940).

Calderbank, P. H., and M. B. Moo-Young, "The Continuous Phase Heat and Mass-Transfer Properties of Dispersions," *Chem. Eng. Sci.*, **16**, 39 (1961).

Chang, S. Y., "Determination of Diffusion Coefficient in Aqueous Solutions," S.M. thesis, Mass. Inst. Technol., Cambridge (1949).

Chilton, T. H., and A. P. Colburn, "Mass Transfer (Absorption) Coefficients. Prediction from Data on Heat Transfer and Fluid Friction," *Ind. Eng. Chem.*, **26**, 1183 (1934).

Colton, C. K., "Permeability and Transport Studies in Batch and Flow Dialyzers with Applications to Hemodialysis," Ph.D. thesis, Mass. Inst. Technol., Cambridge (1969).

———, et al., "Permeability Studies with Cellulosic Membranes," *J. Biomed. Mater. Res.*, **5**, 457 (1971).

Daily, J. W., and R. E. Nece, "Chamber Dimension Effects on Induced Flow and Frictional Resistance of Enclosed rotating Disks," *J. Basic Eng., Trans. ASME, Ser. D*, **82**, 217 (1960).

Dainty, J., "Water Relations of Plant Cells," *Adv. Botan. Res.*, **1**, 279 (1963).

Dorfman, L. A., Hydrodynamic Resistance and the Heat Loss of Rotating Solids, Oliver and Boyd, London (1963).

Eckert, E. R. G., and T. W. Jackson, "Analysis of Turbulent Free Convection Boundary Layer on Flat Plate," Nat. Advisory Comm. Aeronaut. Report 1015 (1951).

Ginzburg, B. Z., and A. Katchalsky, "The Frictional Coefficients of the Flows of Non-Electrolytes Through Artificial Membranes," *J. Gen. Physiol.*, **47**, 403 (1968).

Goldsmith, R. L., "Macromolecular Ultrafiltration with Microporous Membranes," *Ind. Eng. Chem. Fundamentals*, **10**, 113 (1971).

Helfferich, F., "Bi-ionic Potentials," *Disc. Faraday Soc.*, **21**, 83 (1956).

———, Ion Exchange, McGraw-Hill, New York (1962).

Holmes, J. T., C. R. Wilke, and D. R. Olander, "Convective Mass Transfer in a Diaphragm Diffusion Cell," *J. Phys. Chem.*, **67**, 1469 (1963).

Ippen, A. T., "Influence of Viscosity on Centrifugal-Pump Performance," *Trans. ASME*, **68**, 823 (1946).

Johnson, A. I., and C. J. Huang, "Mass Transfer Studies in an Agitated Vessel," *AIChE J.*, **2**, 412 (1956).

Kaufmann, T. G., and E. F. Leonard, "Studies of Intramembrane Transport: A Phenomenological Approach," *ibid.*, **14**, 110 (1968a).

———, "Mechanism of Interfacial Mass Transfer in Membrane Transport," *ibid.*, 421 (1968b).

Von Kiss, A., and A. Urmanczy, "Uber den Mechanismus von Reaktionen, bei welchen die Reaktionskomponenten durch eine Membran Diffundieren," *Z. Anorg. Allegn. Chem.*, **224** 40 (1935).

Kolmogoroff, A. N., "Dissipation of Energy in Locally Isotropic Turbulence," *C.R. Acad. Sci. U.S.S.R.*, **32**, 16 (1941).

La Conti, A. B., J. F. Enos, and C. K. Colton, "Use of Hydrated Polyphenylene Oxide Sulphonate Ion Exchange Membranes for Artificial Kidneys," *Nature*, **230**, 388 (1971).

Lane, J. A., and J. W. Riggle, "Dialysis," *Chem. Engr. Prog. Symp. Ser. No. 24*, **55**, 127 (1958).

Lehmkuhl, G. D., and J. L. Hudson, "Flow and Mass Transfer Near an Enclosed Rotating Disk: Experiment," *Chem. Eng. Sci.*, **26**, 1601 (1971).

Leonard, E. F., and L. W. Bluemle, "Evaluation of Dialysis Membranes," *Trans. Am. Soc. Artificial Internal Organs*, **8**, 182 (1962).

Mackay, D., and P. Meares, "On the Correction for Unstirred Films in Ion-Exchange Membrane Cells," *Kolloid Z.*, **167**, 37 (1959).

Marangozis, J., and A. I. Johnson, "Mass Transfer With and Without Chemical Reaction," *Can. J. Chem. Eng.*, **39**, 152 (1961).

———, "A Correlation of Mass Transfer Data of Solid-Liquid Systems in Agitated Vessels," *ibid.*, **40**, 231 (1962).

Marshall, R. D., and J. A. Storrow, "Dialysis of Caustic Soda Solutions," *Ind. Eng. Chem.*, **43**, 2934 (1951).
Pantell, K., "Versuche über Scheibenreibung," *Forsch. Gebiete Ingenieurw.*, **16**, 97 (1950).
Peterson, M. A., and H. P. Gregor, "Diffusion-Exchange of Ions and Nonexchange Electrolyte in Ion-Exchange Membrane Systems," *J. Electrochem. Soc.*, **106**, 1051 (1959).
Phipps, D. L., Jr., "Mass Transfer in a Mechanically Agitated Batch Dialyzer," S.M. thesis, Mass. Inst. Technol., Cambridge (1967).
Rogers, M. H., and G. N. Lance, "The Boundary Layer on a Disc of Finite Radius in a Rotating Fluid," *Quart J. Mech. Appl. Math.*, **17**, 319 (1964).
Scattergood, E. M., "Electrokinetic Membrane Processes," Ph.D. thesis, Univ. of Wisconsin, Madison (1966).
———, and E. N. Lightfoot, "Diffusional Interaction in an Ion-Exchange Membrane," *Trans. Faraday Soc.*, **64**, 1135 (1968).
Schultz-Grunow, F., "Der Reibungswiderstand rotierender Scheiben in Gehäusen," *Z. angew. Math. Mech.*, **15**, 191 (1936).
Seidell, A., Solubilities of Inorganic and Metal Organic Compounds, 3rd ed., Van Nostrand, New York (1940).
Smith, K. A., et al., "Convective Transport in a Batch Dialyzer: Determination of True Membrane Permeability from a Single Measurement," *Chem. Eng. Progr. Symp. Ser. No. 84*, **64**, 45 (1968).
Smith, K. A., and C. K. Colton, "Mass Transfer to a Rotating Fluid. Part I. Transport from a Stationary Disk to a Fluid in Bödewadt Flow," *AIChE J.*, **18**, 949 (1972).
Soo, S. L., "Laminar Flow Over an Enclosed Rotating Disk," *Trans. ASME*, **80**, 287 (1958).
Stokes, R. H., "An Improved Diaphragm-cell for Diffusion Studies, and Some Tests of the Method," *J. Am. Chem. Soc.*, **72**, 763 (1950).
Tomlan, P. F., and J. L. Hudson, "Flow Near an Enclosed Rotating Disk: Analysis," *Chem. Eng. Sci.*, **26**, 1591 (1971).
Wilson, E. E., "A Basis for Rational Design of Heat Transfer Apparatus," *Trans. ASME*, **37**, 47 (1915).

Manuscript received November 24, 1971; revision received May 19, 1972; paper accepted May 19, 1972.

Using the Dusty Gas Diffusion Equation in Catalyst Pores Smaller than 50 Å Radius

When the dusty gas diffusion equation is applied to materials containing pores with radii below 50 Å, the observed diffusion behavior in these smaller pore systems can be quite different from that predicted by the equation. Higher temperatures and in some cases higher pressures tend to lessen the deviations between prediction and experiment. The observed deviations are probably caused by surface transport and by momentum transfer between gas molecules and pore walls during molecular flight. For bimodal materials, an additional factor can be the inapplicability of the equation to systems of parallel micro- and macropores. Excellent agreement between theory and experiment occurs for large-pore unimodal systems.

HIROKAZU OMATA and LEE F. BROWN

Department of Chemical Engineering
University of Colorado
Boulder, Colorado 80302

SCOPE

Diffusion and bulk transport of gases and liquids within porous materials can be of critical importance in catalysis, adsorption, and separation processes. Within recent years, investigation of the diffusion and transport of gases within porous materials has resulted in increasingly effective and rigorous correlation and prediction techniques. The heart of these techniques has been the so-called "dusty gas diffusion equation," independently derived by three sets of investigators. This equation covers the entire range from Knudsen diffusion through the transition region into bulk or molecular diffusion and as a result gives promise of extremely wide applicability to gaseous diffusion within porous materials under all types of process conditions.

Under the two limiting conditions of Knudsen diffusion and bulk diffusion and flow, equations have long existed which gave useful agreement between theory and experiment. But until the development of the dusty gas equation, mass transport in the transition region was not as well described. This was a critical lack because the transition region covers a wide range of pore sizes and process conditions. Using the dusty gas equation, Satterfield (1970) gave the range of pore sizes within the transition region for some binary gas mixtures at 300°C. and 1 atm. He listed pores as small as 8 Å and as large as 26,300 Å as lying within the transition region, depending on the gas composition. These sizes encompass the pores in most porous catalysts and adsorbents, with the exception of some molecular sieves and active carbons.

Thus the dusty gas equation appears to be necessary for describing gas-phase transport within a large number

Correspondence concerning this paper should be addressed to L. F. Brown. H. Omata is at #272 Hachimanmae-shataku, Mitsui Toatsu Chemicals, Inc., Mobara-shi, Chiba-ken, Japan.